NIH Public Access
Author Manuscript
Invest Ophthalmol Vis Sci. Author manuscript; available in PMC 2009 March 31.

Published in final edited form as:
Invest Ophthalmol Vis Sci. 2007 February ; 48(2): 881–890. doi:10.1167/iovs.06-0723.

Gene Expression Profiling of Zebrafish Embryonic Retina

YUK FAI LEUNG and **JOHN E. DOWLING**
Department of Molecular and Cellular Biology, Harvard University, Cambridge, Massachusetts

Abstract

A methodology for microdissecting intact retinas from zebrafish embryos at early developmental stages for expression profiling was developed in this study. Total RNA was extracted consistently and reproducibly from the dissected retinas using a customized extraction protocol. The results from microarray experiments indicated that the purified RNA samples faithfully represented the biological differences among different types of samples. Genes that were differentially expressed in a particular neuronal layer or region of the retina were detectable by microarray experiments. In conclusion, this methodology makes it possible to obtain retinal-specific total RNA for genomics research on retinal development in zebrafish.

INTRODUCTION

Zebrafish have become a pre-eminent vertebrate model system in recent years.[1,2] Several studies on the genetics of its development have utilized large-scale mutagenesis approaches to find causative genes for particular mutant phenotypes.[3] The molecular function of an identified gene needs to be characterized to correlate it to the observed phenotype. However genes are not isolated entities; they work together in a complex network to control various molecular and cellular processes. Mutations in one gene can affect the expression of many other genes, and in turn the activity of their protein products. Therefore, it is advantageous to study the gene expression profile of a mutant, and to compare it with its wild-type counterpart to fully understand the effects of a mutation. Studying the change in gene expression profiles in a time series experiment can often give insights into the genetic networks that control various developmental processes.

Unfortunately, gene expression profiling in multicellular organisms is complicated by large differences in gene expression in different parts of the body. Further, a mutation can alter gene expression in different tissues in different ways. For retinal development studies in animal model systems such as mouse or in humans, this problem is circumvented by dissecting the retinas out of embryos, and performing expression profiling on the total RNA extracted from the retina alone by RT-PCR, or high-throughput approaches like serial analysis of gene expression (SAGE)[4–6] or microarrays.[7,8] To date, there has not been a large-scale gene expression study of retinal development in zebrafish primarily because the embryo is so small when retinal development and differentiation take place. There have been a few zebrafish microarray studies in which a target tissue was dissected out from 6 dpf embryos,[9] or a minimal dissection of the embryos was performed to obtain the distal part of the body trunk before total RNA extraction.[10] However, most microarray studies of zebrafish have either used adult tissues[11–13] or whole embryos[14–17] for total RNA extraction. In developmental studies, the expression information obtained from whole-embryo samples is merely an average value, and may not represent the real biological change in the target tissue. During retinal development,

Address reprint requests to: Yuk Fai Leung, Department of Molecular and Cellular Biology, Harvard University, 16 Divinity Avenue, Cambridge, MA 02138, E-mail: yfleung@mcb.harvard.edu.

NIH-PA Author Manuscript
NIH-PA Author Manuscript
NIH-PA Author Manuscript

NIH-PA Author Manuscript
NIH-PA Author Manuscript
NIH-PA Author Manuscript

many genes express specifically in the retina or even a specific layer of the retina. These genes may also have a differential expression pattern in the retina, or have complex temporal and spatial regulation patterns as compared with the rest of the body. Hence it is crucial to dissect the retina out cleanly from the zebrafish embryo in order to perform a meaningful gene expression profiling of retinal development.

The focus of the present study was first to establish a microdissection protocol for the developing and differentiating zebrafish embryonic retina, followed by a customized total RNA extraction procedure for gene expression profiling. A microarray-based comparison between wild-type retinal and whole-embryo samples was performed using purified total RNAs. The microarray expression profiling detected subtle gene expression changes even in single neuronal layers or particular regions of the retina. The results suggest that this protocol is reproducible, consistent, and suitable for studying retinal development in zebrafish.

MATERIALS AND METHODS

Fish

Zebrafish were maintained according to standard procedures.[18] The AB wild-type line was used in this study.

Egg Collection, Embryo Staging and Collection

To ensure that all embryos were at the same stage to facilitate subsequent dissection, the parent fish were separated and allowed to cross every other hour for 10 minutes. It was possible to collect embryos up to five times in a single day in this way. About forty eggs were collected during each cross.

Zebrafish embryo staging was done according to Kimmel et al.,[19] and eye diameter measurements made as described below. All embryos were first staged at around 10–12 hours post-fertilization (hpf) (tailbud to four somites). Only those embryos at the same stage in the same collection were kept for downstream dissection. The embryos were staged again at 36 and 52 hpf, immediately before dissection.

Eye diameters at 36 and 52 hpf were estimated by imaging fifty to sixty staged embryos from a single clutch as they lay in the Petri dish. The eye diameter was defined as the longest length of the developing eye, the measurement performed by ImageJ (http://rsb.info.nih.gov/ij/). Eight such clutches were collected and measured independently, so that the total number of embryonic eyes measured was about four hundred. The population means of the eye diameters, estimated from the means of eight replicates, were determined to be 220.6 μm for 36 hpf (95% CI = 215.0 μm—226.2 μm) and 266.8 μm for 52 hpf (95% CI = 261.2 μm—271.7 μm).

During the actual dissection, the eye diameter of the embryos was measured by the calibrated scale in the eyepiece of the dissection microscope. Only those embryos whose eye diameters fell within the 95% confidence intervals (CIs) of the population mean, and fulfilled the conventional staging criteria, were chosen for final dissection.

For the total RNA extraction experiments, five staged embryos were collected in 225 μL TRIzol reagent (Invitrogen, Carlsbad, CA) in an RNase-free microtube (VWR International, West Chester, PA). The solution was vortexed vigorously for 1 minute to disrupt the embryos, and then stored at −80°C before total RNA extraction.

NIH-PA Author Manuscript

NIH-PA Author Manuscript

NIH-PA Author Manuscript

Dissection

Zebrafish embryos were maintained at 28°C on a heated block before dissection. The embryo was transferred to Ringer's solution[18] in a Falcon 60 × 15 mm polystyrene culture plate for dissection (BD Biosciences, San Jose, CA). The basic dissection was done with a pair of Dumont #55 forceps (Tips: 0.05 × 0.01 mm) (World Precision Instrument, Sarasota, FL) with another pair of Dumont #5 forceps (Tips: 0.025 × 0.015 mm; World Precision Instrument) holding the embryos. Fine manipulations were done with a tungsten needle chemically etched from tungsten wire, 0.015 inch in diameter (World Precision Instrument).

The embryo head with part of the anterior trunk was cut off from the body (Fig. 1A). A hole was punched in the forehead by the tip of the Dumont #55 forceps, with another forceps pining the head on the Petri dish (Fig. 1B, steps 1 and 2). The head was opened on the dorsal side up to the posterior end of the otic vesicle (Fig. 1B, steps 2 and 3). The brain was removed so that the medial side of the eyes faced upward (Fig. 1C, step 1).

The retinal pigment epithelium (RPE) was removed with the eye still largely attached to the skin. The head was pinned to the Petri dish roughly through the otic vesicle area by the assistant forceps (Fig. 1C, step 2). The RPE was carefully brushed by the tip of the Dumont #55 forceps (Fig. 1C, step 3) until a small opening to the retina was seen (Figs. 1D, 2A and B). Further brushing and peeling were done only on the unopened RPE (Fig. 1D) until the medial side of the retina, which faced upward during the dissection, was almost all exposed (Fig. 1E). It was not necessary to remove the residual RPE on the medial side at this stage because it was removed subsequently by selective adherence to the surface of a Petri dish (see below). However, care was taken not to open more than one hole, as the RPE cells between two holes became an imbedded fine string of cells when the holes were further opened. Such a string of cells was very difficult to remove and disrupted the integrity of the retina when buried deep into the tissue.

The lateral RPE, which was facing downward, was removed by inserting the tip of the Dumont #55 forceps at an angle of approximately 45° from the Petri dish surface (Fig. 1E, step 1) and brushing in an anticlockwise motion (Fig. 1E, steps 2 and 3). The RPE which attached firmly to the ora serrata was largely removed by pinning it to the Petri dish using the assistant forceps (Fig. 1F, step 1), and then lifting the retina using the tip of Dumont #55 forceps gently (Fig. 1F, step 2).

The retina was then rolled on the bottom of the Petri dish to clean up the residual RPE (Fig. 1G). For approximately 20 minutes after the initial addition of the Ringer's solution, the RPE cells adhered preferentially to the Petri dish. The retinal cells also attached to the Petri dish but to a lesser extent; thus a balance was struck between cleanliness and integrity of the retina. In practice, most RPE could be removed without observable damage to the retina. During the rolling process, the lens often adhered to the Petri dish and detached from the retina. Occasionally, it was necessary to detach the lens by an etched tungsten needle of 10–15 μm tip diameter with a swirling motion in the centre of the lens (Figs. 1H and 1I, 2C and D).

Retinas were successfully dissected from live embryos at 36 and 52 hpf using this methodology (Fig. 3). It took approximately 15 minutes to stage and dissect one retina from an embryo. Most of the dissection time was devoted to the removal of the RPE. The dissected retinas were largely devoid of RPE contamination. However, some RPE remnants remained in the ora serrata region, where RPE cells could not encounter the adhering surface of the Petri dish. In many cases, the earlier lifting action (Fig. 1F, step 2) removed most of these cells. Also, the RPE remnants appeared to be damaged rather than intact cells; therefore their presence should not greatly affect gene expression measurement.

NIH-PA Author Manuscript

NIH-PA Author Manuscript

NIH-PA Author Manuscript

The dissected retina was put immediately into 300 μL ice-cold TRIzol in an RNase-free microtube (VWR International, West Chester, PA), and the solution was shaken to disrupt the cells. Usually three or four retinas were collected in the same tube, and the final mixture was further vortexed for 1 minute. The samples were stored at −80°C before total RNA extraction.

Total RNA Extraction and Quality Check

All procedures were done using RNase-free reagents and tubes. All tools were thoroughly cleaned with RNase Away (Molecular Bio-Products Inc., San Diego, CA).

Homogenization

Total RNA extraction was done by combining TRIzol and a column-based extraction procedure. For whole-embryo samples, two tubes of the same type of sample in 225 μL of TRIzol were combined to give a total volume of 450 μL. The sample was homogenized by pestling with an RNase free Pestle (VWR International) about 100 times until the solution became homogeneous. The pestle was then washed with 150 μL fresh TRIzol and mixed with the 450 *3*L mixture to give a final sample volume of 600 μL. For retinal samples, three tubes of the same type of sample in 300 μL TRIzol were individually pestled to avoid spilling, and then combined to give a total volume of 900 μL. The pestle was finally washed with 100 μL fresh TRIzol and mixed with the 900 μL mixture to give a final sample volume of 1000 μL. The sample was further homogenized by spinning through a QIAshredder column (Qiagen, Valencia, CA) at full speed for 2 minutes. The resultant lysate was incubated at room temperature for 5 minutes. The debris in the mixture was spun down by spinning at 12,000 *g* for 10 minutes at 4°C. The supernatant was transferred to a new microcentrifuge tube.

TRIzol Extraction and Aqueous Phase Separation

One-fifth volume of chloroform (Sigma-Aldrich, St. Louis, MO) was added to the sample (whole-embryo:120 μL, retina: 200 μL). The mixture was vortexed for 1 minute and then incubated at room temperature for another 3 minutes. The clear aqueous phase was completely separated from the red organic phase by spinning at 16,000 *g* for 5 minutes at 4°C in a prespun Phase Lock Gel (PLG) tube (Eppendorf, Hamburg, Germany). The clear aqueous layer, which was about sixty percent of the starting volume, was transferred to a new microcentrifuge tube, and re-extracted with an equal volume of chloroform. The mixture was again incubated at room temperature for 3 minutes, and the aqueous phase separated from the organic phase using a new PLG tube as mentioned before. The volume of the aqueous layer usually reduced by about ten percent after the second extraction.

Column Purification

An equal volume of 70% ethanol in diethylpyrocarbonate (DEPC)-treated water (Ambion, Austin, TX) was added to the aqueous layer and mixed immediately by pipetting. The mixture was loaded on an RNeasy MinElute Cleanup column (Qiagen) in a 700 μL portion, and bound to the membrane by spinning at 8000 *g* for 15 seconds. The sample was washed with 700 μL buffer RPE three times, with a 5-minute incubation for the first two washes before spinning. The sample was finally washed by 700 μL 80% ethanol in DEPC-treated water, and spun at 8000 *g* for 2 minutes. The column was dried by spinning at full speed for another 5 minutes with the cap opened. The RNA was eluted by adding 14 μL of DEPC-treated water to the column membrane, and spun at full speed for 1 minute. The typical elution volume was about 12.6 μL for retinal samples and 11.6 μL for whole-embryo samples.

RNA Quality Measurement

The yield and the purity of the extracted total RNAs were evaluated by measuring the ultraviolet (UV) absorbance in a Nanodrop spectrophotometer (NanoDrop Technologies, Wilmington,

NIH-PA Author Manuscript

NIH-PA Author Manuscript

NIH-PA Author Manuscript

DE), and electrophoresing 1 μL of the eluant in an RNA 6000 Nano LabChip running in a 2100 Bioanalyzer (Agilent Technologies, Palo Alto, CA).

Microarray Experiment and Analysis

The total RNAs extracted from retinal and stage-matched whole-embryo samples were amplified by a modified Eberwine protocol,[20] as implemented in an Affymetrix two-cycle target labeling protocol (Affymetrix, Santa Clara, CA), and hybridized to Affymetrix GeneChip Zebrafish Whole Genome Arrays (Affymetrix). All hybridization, washing, and scanning were done according to a standard procedure from Affymetrix. The probe-level data were background adjusted, normalized and summarized by a Robust Multi-array Average (RMA) algorithm[21] implemented in the software package affy of the Bioconductor project release 1.6 (http://www.bioconductor.org), running in the R statistical environment version 2.1.0 (http://www.r-project.org) using default parameters. A fold change of each gene was calculated for the comparison of wild-type retinal and whole-embryo samples at 52 hpf, based on an average of the summarized expression levels of the three biological replicates of each condition.

RESULTS

RNA Quality

Typical UV absorbance and bioanalyzer electrophoretic profiles of the whole-embryo and retina samples are shown in Figure 4. The profiles are virtually identical to the samples that were collected in either TRIzol or RNAlater (Ambion, Austin, TX), and extracted immediately after collection (data not shown). These results suggested a short-term storage of samples in ice bath during dissection did not compromise the total RNA quality.

In a first microarray study of retinal development and differentiation in zebrafish, ten retinas were dissected from wild-type embryos at 36 and 52 hpf. Ten stage-matched whole embryos were also collected as controls. Three biological replicates were collected for each type of sample, and they were extracted independently. Typical RNA yields for different types of samples are shown in Figures 5A and 5B. Approximately 0.5–0.6 μg total RNA could be extracted from each embryo. The retina at 36 and 52 hpf gave roughly the same amount of total RNA. On average, 17.9 ± 2.3 ng of total RNA was obtained from each retina. The conventional 260/280 absorbance and 28s/18s ribosomal peak ratios were not a consistent quality measure for the retina samples, as their yield was very low. For the whole-embryo samples, the present procedure gave an average 260/280 ratio of 2.03 ± 0.06, and 28s/18s ratio of 1.68 ± 0.08. The ultimate consistent quality measure was found to be the bioanalyzer electrophoretic profile. Total RNAs with a clean baseline and intact ribosomal peaks as shown in Figures 4C and 4D always gave good results.

Microarray Analysis

In the microarray experiment, 33 ng of the total RNA from each sample was used for the labeling reaction. The three biological replicates were labeled independently. Figure 5C shows the pairwise correlation coefficients among the three biological replicates, using the Perfect-Match (PM) probe intensities (circles) and normalized intensities (triangles). PM intensities are unaltered raw data and are comprised of gene specific signal, systematic and random errors, while the normalized intensities are comprised of gene specific signal and random errors. In this experiment, the pairwise correlation coefficient were at least 0.966 and 0.985 for raw and normalized data, respectively. Apparently, the systematic errors introduced by various experimental manipulations did not contribute to a significant variation in the data. A scatterplot of biological replicate 1 and 3 of WA36 sample gives an idea of the actual correlation between them (Fig. 5D). In this plot, 249752 PM probe intensities are shown and mostly lie

NIH-PA Author Manuscript

NIH-PA Author Manuscript

NIH-PA Author Manuscript

on the diagonal line, suggesting the methodology can give RNA of consistent and reproducible quality.

A comparison of wild-type retinal to whole-embryo samples at 52 hpf (WR52/WA52) was performed using the microarray data. Twenty most overexpressed and underexpressed annotated genes as judged by fold change are shown in Table 1. The corresponding comparisons of the retinal samples at 52 and 36 hpf (WR52/WR36), Gene Ontology (GO) annotations, and zfin IDs are also listed in the table. The overexpressed genes in the retina at 52 hpf are mostly transcription factors that control retinal development and differentiation (e.g., *pax6b*, *six7*, *ndrg1l*, *atoh7*, *junb*, *prox1*), or components of visual signal transduction cascade (e.g., *rem1*, *rlbp1l*, *rho*, *aanat2*, *gngt2*, *arl3l1*). Almost all genes that were underexpressed in the retina, or overexpressed in the whole embryo at 52 hpf code for structural proteins for muscle and its development (*myhz2*, *Tnni2*, *tnnt3b*, *myhc5*, *postn*, *acta1*, *pvalb1*, *tpma*), mediators for muscle contractions (e.g., *atp2a1*, *tnnc*), or other structural proteins (e.g., *cyt1*, *krt4*, *col1a1*).

DISCUSSION

This study successfully established a microdissection procedure for obtaining pure and intact embryonic retinas from zebrafish embryos at 36 and 52 hpf. The dissection methodology was also tested on 3 dpf embryos with success. The RPE was much harder to remove at 3 dpf, and a slightly longer time for dissection was necessary. Although the dissection methodology has never been systematically tested on embryonic stages earlier than 36 hpf, it is believed that this dissection procedure is applicable to earlier developmental stages.

Ringer's solution[18] was used as a medium for dissection because it is a commonly used solution for electrophysiology, and retinal cells can be maintained in their functional state in Ringer's solution for an extended period of time.[22] This ensured that retinal integrity and retinal gene expression were not altered by the change in the environment during dissection. In addition, both retinas can be dissected from the same embryo without any effects on RNA integrity, as judged by the bioanalyzer profile (data not shown). The brushing action that was used to open the RPE unavoidably created some damage on the retina. However, it is believed the photoreceptor layer was largely intact, because most RPE was peeled off with the brushed area, and hence the retina was mostly free of damage. The integrity of the retina is supported by the intactness of the gross morphology of the photoreceptor layer after dissection (Figs. 2C and D), and the detection of photoreceptor specific gene expression in the retina total RNA samples by the microarray experiments as described below. Even though there might be some unobservable damage in one retina, the pooling of several retinas in one sample should be able to ameliorate the situation, as the small damage in one retina was not likely to present in the same place in another retina.

The RNA remained stable in TRIzol solution when stored on ice during dissection, and at −80° C for 3 months after collection, as indicated by identical bioanalyzer profiles of such samples when compared to samples collected and extracted immediately. This also suggests that snap-freezing is not necessary. A high pairwise correlation coefficient between biological replicates in the microarray experiment further suggests that this methodology is reproducible and consistent. Moreover, the extracted RNAs faithfully represent the real biological differences between different types of samples, as demonstrated by the tissue-specific gene expression pattern between wild-type retinal and whole-embryo samples at 36 and 52 hpf. This pattern is further supported by *in situ* hybridization data available in the zfin database (http://zfin.org). There are *in situ* images for eleven out of the twenty overexpressed genes in the retina, and thirteen out of the twenty underexpressed genes in the retina from Prim-15 (30–36 hpf) to Prim-25 (36–42 hpf), and High-pec (42–48 hpf) to Long-pec (48–60 hpf) stage. At 52 hpf, all

NIH-PA Author Manuscript

NIH-PA Author Manuscript

NIH-PA Author Manuscript

eleven overexpressed genes are observed throughout the retina (*pax6b*, *ndrg1l*, *vsx1*), or in a particular cell layer or region of the retina (*proml2*, *rem1*, *rlbp1l*, *rho*, *gngt2*, *arl3l1*, *junb*, *ca7*); while all thirteen underexpressed genes (*myhz2*, *atp2a1*, *tnnt3b*, *acta1*, *pvalbl*, *cyt1*, *tfa*, *krt4*, *tnnt3a*, *cfl1*, *col1a1*, *cldni*, *ckm*) are observed more prominently in body parts other than retina. Interestingly, *rho, gngt2* and *arl3l1* are specifically expressed in the photoreceptor layer, further supporting the intactness of the retina during the RPE removal process.

The corresponding comparisons of gene expression in the retina at 52 and 36 hpf (WR52/WR36) are also supported by the *in situ* hybridization data in zfin. In particular, all eleven overexpressed genes mentioned above have a corresponding time-dependent increase. For the thirteen underexpressed genes, all except *myhz2* and *krt4* have the corresponding *in situ* data at 36 hpf, in which the expression of the genes does not change over time. Even for *myhz2* and *krt4*, the *in situ* data available for time points earlier than 36 hpf show that there is no expression of them in retina throughout development. Therefore, it is very likely that the thirteen underexpressed genes are not expressed in retina at all, and thus they don't have a time-dependent change. The expression of *atoh7/ath5* decreases over time, as suggested by the microarray result. Although there is no *in situ* data from zfin, this time-dependent decrease was previously reported.[23,24] In short, the *in situ* hybridization data support the microarray results obtained in the present study.

The availability of total RNAs from the developing retinas makes it possible to perform a genome-scale study of retinal development in zebrafish. The resolution of gene expression, as shown by the microarray result, is to a particular neuronal layer or restricted region of the retina. This indicates that even a subtle change in gene expression in the retina is very likely to be measurable by microarray analysis. Currently a large-scale microarray project is in progress, using wild-type samples as shown in Figure 3 and stage-matched samples collected from a retinal lamination mutant called *young*,[25,26] with the aim to identify genes that control retinal development and differentiation.

The results from such comprehensive genome-scale studies could complement the information obtained by existing technologies including *in situ* hybridization and immunohistochemistry, which give discrete spatial and temporal expression information of a gene and its protein product. The information could also further our understanding of the continuous dynamical expression data obtained by in vivo imaging of transgenic animals. A well-designed genomic screening can also prioritize candidate genes for functional validation by morpholino microinjection. The integration of all these approaches not only have made the functional genomics research of retinal development in zebrafish possible, but also positioned it as a unique multicellular vertebrate model that is extremely suitable for systems biology research.

Acknowledgements

This work was supported by The Merck Award for Genomics Research, The Croucher Foundation Postdoctoral Fellowship Research Allowance, and The NEI grant EY00811. Yuk Fai Leung was supported by The Croucher Foundation Postdoctoral Fellowship.

The authors thank Ellen A. Schmitt for her advice on animal staging and microdissection procedures; Brian A. Link for his help on studying the *yng* mutant; Edward Fox, Peter Hoyt, John Ngai, and John Rawls for their valuable comments on total RNA extraction and RNA quality evaluation; Jennifer Couget and ShuFen Meng for their excellent support on Affymetrix GeneChip experiment; Ping Ma for his expert advice on data analysis; Chi Kong Yeung for his critical comments on the manuscript; and members from Dowling lab for helpful discussions.

References

1. Grunwald DJ, Eisen JS. Headwaters of the zebrafish—emergence of a new model vertebrate. Nat Rev Genet 2002;3:717–724. [PubMed: 12209146]

NIH-PA Author Manuscript

NIH-PA Author Manuscript

NIH-PA Author Manuscript

2. Rasooly RS, Henken D, Freeman N, Tompkins L, Badman D, Briggs J, et al. Genetic and genomic tools for zebrafish research: the NIH zebrafish initiative. Dev Dyn 2003;228:490–496. [PubMed: 14579387]

3. Patton EE, Zon LI. The art and design of genetic screens: zebrafish. Nat Rev Genet 2001;2:956–966. [PubMed: 11733748]

4. Blackshaw S, Fraioli RE, Furukawa T, Cepko CL. Comprehensive analysis of photoreceptor gene expression and the identification of candidate retinal disease genes. Cell 2001;107:579–589. [PubMed: 11733058]

5. Blackshaw S, Harpavat S, Trimarchi J, Cai L, Huang H, Kuo WP, et al. Genomic analysis of mouse retinal development. PLoS Biol 2004;2:E247. [PubMed: 15226823]

6. Sharon D, Blackshaw S, Cepko CL, Dryja TP. Profile of the genes expressed in the human peripheral retina, macula, and retinal pigment epithelium determined through serial analysis of gene expression (SAGE). Proc Natl Acad Sci USA 2002;99:315–320. [PubMed: 11756676]

7. Livesey FJ, Furukawa T, Steffen MA, Church GM, Cepko CL. Microarray analysis of the transcriptional network controlled by the photoreceptor homeobox gene Crx. Curr Biol 2000;10:301–310. [PubMed: 10744971]

8. Diaz E, Yang YH, Ferreira T, Loh KC, Okazaki Y, Hayashizaki Y, Tessier-Lavigne M, et al. Analysis of gene expression in the developing mouse retina. Proc Natl Acad Sci USA 2003;100:5491–5496. [PubMed: 12702772]

9. Rawls JF, Samuel BS, Gordon JI. Gnotobiotic zebrafish reveal evolutionarily conserved responses to the gut microbiota. Proc Natl Acad Sci USA 2004;101:45964601.

10. Leung AY, Mendenhall EM, Kwan TT, Liang R, Eckfeldt C, Chen E, et al. Characterization of expanded intermediate cell mass in zebrafish chordin morphant embryos. Dev Biol 2005;277:235–254. [PubMed: 15572152]

11. Malek RL, Sajadi H, Abraham J, Grundy MA, Gerhard GS. The effects of temperature reduction on gene expression and oxidative stress in skeletal muscle from adult zebrafish. Comp Biochem Physiol C Toxicol Pharmacol 2004;138:363–373. [PubMed: 15533794]

12. Meijer AH, Verbeek FJ, Salas-Vidal E, Corredor-Adamez M, Bussman J, van der Sar AM, et al. Transcriptome profiling of adult zebrafish at the late stage of chronic tuberculosis due to *Mycobacterium marinum* infection. Mol Immunol 2005;42:1185–1203. [PubMed: 15829308]

13. van der Ven K, De Wit M, Keil D, Moens L, Van Leemput K, Naudts B, et al. Development and application of a brain-specific cDNA microarray for effect evaluation of neuroactive pharmaceuticals in zebrafish *(Danio rerio)*. Comp Biochem Physiol B Biochem Mol Biol 2005;141:408–417. [PubMed: 15979371]

14. Ton C, Stamatiou D, Liew CC. Gene expression profile of zebrafish exposed to hypoxia during development. Physiol Genomics 2003;13:97–106. [PubMed: 12700360]

15. Linney E, Dobbs-McAuliffe B, Sajadi H, Malek RL. Microarray gene expression profiling during the segmentation phase of zebrafish development. Comp Biochem Physiol C Toxicol Pharmacol 2004;138:351–362. [PubMed: 15533793]

16. Thorpe CJ, Weidinger G, Moon RT. Wnt/beta-catenin regulation of the Sp1-related transcription factor sp5l promotes tail development in zebrafish. Development 2005;132:1763–1772. [PubMed: 15772132]

17. Sumanas S, Jorniak T, Lin S. Identification of novel vascular endothelial-specific genes by the microarray analysis of the zebrafish cloche mutants. Blood 2005;106:534–541. [PubMed: 15802528]

18. Westerfield, M. A guide for the laboratory use of zebrafish (*Danio rerio*). Vol. 4. Univ. of Oregon Press; Eugene: 2000. The zebrafish book.

19. Kimmel CB, Ballard WW, Kimmel SR, Ullmann B, Schilling TF. Stages of embryonic development of the zebrafish. Dev Dyn 1995;203:253–310. [PubMed: 8589427]

20. Van Gelder RN, von Zastrow ME, Yool A, Dement WC, Barchas JD, Eberwine JH. Amplified RNA synthesized from limited quantities of heterogeneous cDNA. Proc Natl Acad Sci USA 1990;87:1663–1667. [PubMed: 1689846]

21. Irizarry RA, Hobbs B, Collin F, Beazer-Barclay YD, Antonellis KJ, Scherf U, et al. Exploration, normalization, and summaries of high density oligonucleotide array probe level data. Biostatistics 2003;4:249–264. [PubMed: 12925520]

NIH-PA Author Manuscript

NIH-PA Author Manuscript

NIH-PA Author Manuscript

22. Redenti S, Chappell RL. Zinc chelation enhances the zebrafish retinal ERG b-wave. Biol Bull 2002;203:200–202. [PubMed: 12414577]

23. Masai I, Stemple DL, Okamoto H, Wilson SW. Midline signals regulate retinal neurogenesis in zebrafish. Neuron 2000;27:251–263. [PubMed: 10985346]

24. Kay JN, Link BA, Baier H. Staggered cell-intrinsic timing of ath5 expression underlies the wave of ganglion cell neurogenesis in the zebrafish retina. Development 2005;132:2573–2585. [PubMed: 15857917]

25. Link BA, Fadool JM, Malicki J, Dowling JE. The zebrafish young mutation acts non-cell-autonomously to uncouple differentiation from specification for all retinal cells. Development 2000;127:2177–2188. [PubMed: 10769241]

26. Gregg RG, Willer GB, Fadool JM, Dowling JE, Link BA. Positional cloning of the young mutation identifies an essential role for the Brahma chromatin remodeling complex in mediating retinal cell differentiation. Proc Natl Acad Sci USA 2003;100:6535–6540. [PubMed: 12748389]

NIH-PA Author Manuscript
NIH-PA Author Manuscript
NIH-PA Author Manuscript

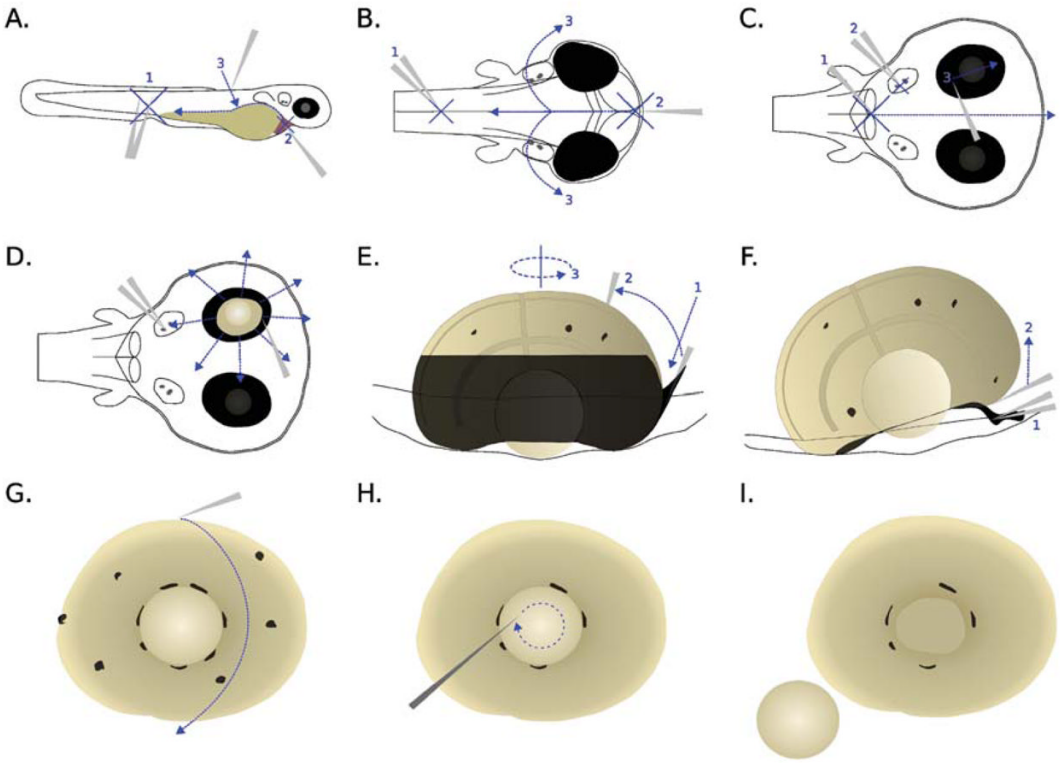

FIG. 1.
Dissection procedures for zebrafish embryonic retina. Refer to text for details.

NIH-PA Author Manuscript
NIH-PA Author Manuscript
NIH-PA Author Manuscript

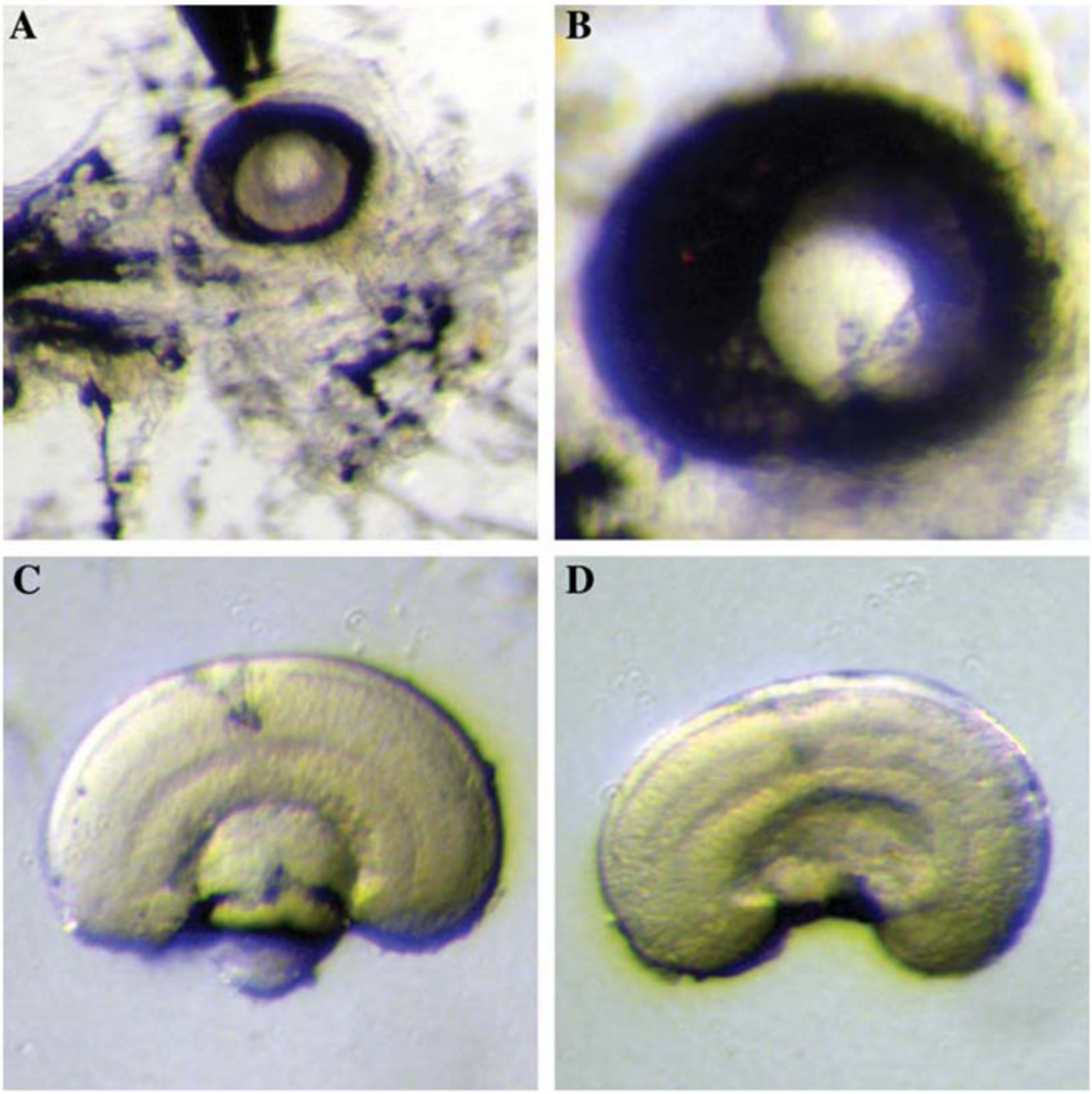

FIG. 2.

Dissection of zebrafish embryonic retina. (**A**) The removal of RPE. The anterior side of the embryo is facing right and the dorsal side is facing upward. The RPE is partially opened and cleaned up from the medial side. (**B**) A higher magnification of the eye with the same orientation as in (A), with RPE partially cleaned-up. (**C**) Dissected retina before the removal of the lens, observed from the side. (**D**) Dissected retina after the removal of the lens, observed from the side. Note that the cell and plexiform layers, as well as the optic nerve, are apparent after the RPE is peeled off.

NIH-PA Author Manuscript

NIH-PA Author Manuscript

NIH-PA Author Manuscript

FIG. 3.

Dissection of wild-type retinas at 36 and 52 hpf. The retinas were dissected from embryos staged at 36 and 52 hpf. Lens and retinal pigment epithelium were removed. Scale bar = 100 μm.

NIH-PA Author Manuscript

NIH-PA Author Manuscript

NIH-PA Author Manuscript

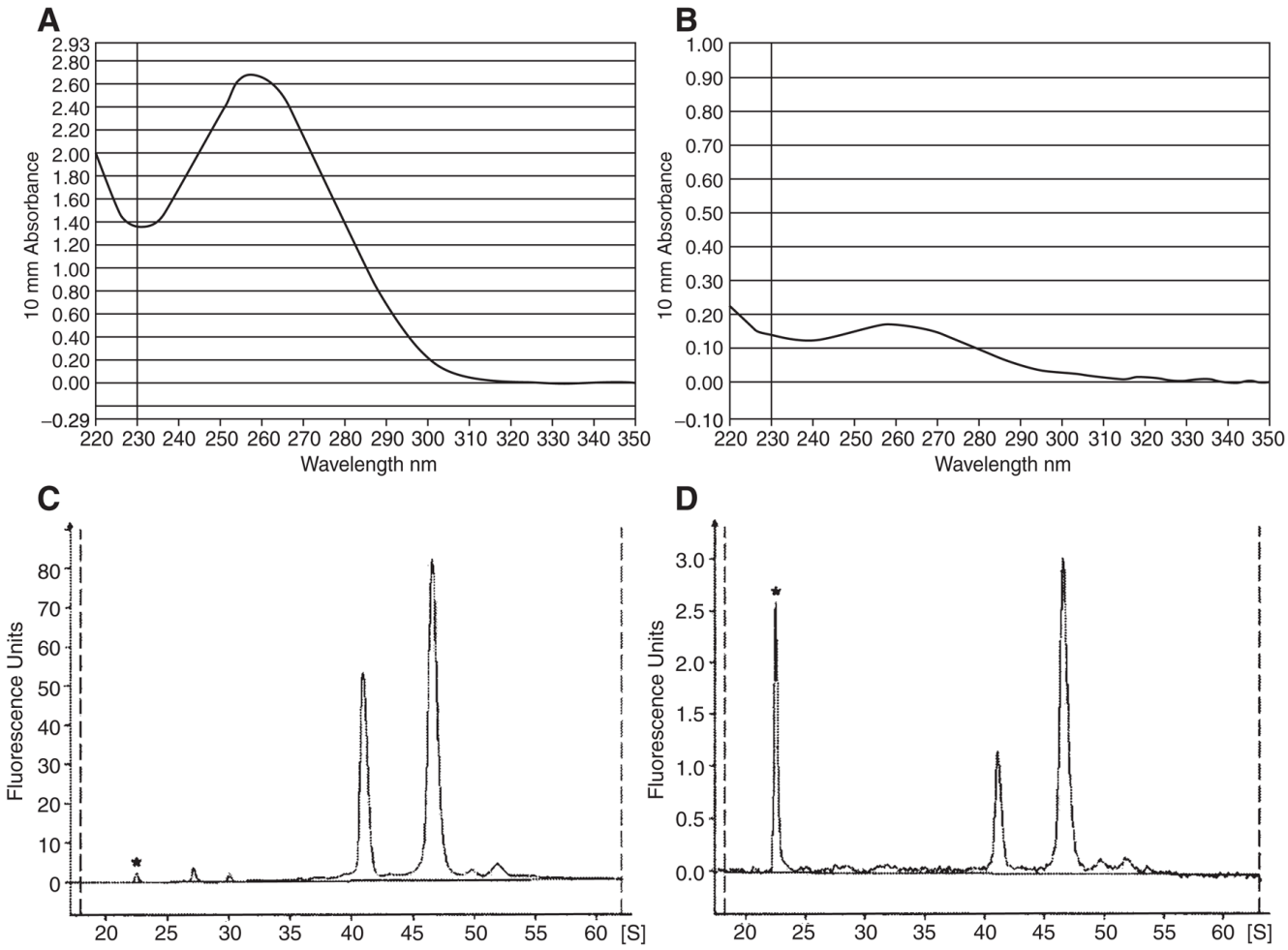

FIG. 4.

Typical UV absorbance and bioanalyzer profiles of total RNA extracted from whole-embryos and retinas sample. (**A**) Typical UV absorbance profile of total RNA extracted from ten embryos. (**B**) Typical UV absorbance profile of total RNA extracted from ten retinas. (**C**) Typical bioanalyzer profile of total RNA extracted from ten embryos. (**D**) Typical bioanalyzer profile of total RNA extracted from ten retinas. The peaks with an asterisk are the internal size standard.

NIH-PA Author Manuscript

NIH-PA Author Manuscript

NIH-PA Author Manuscript

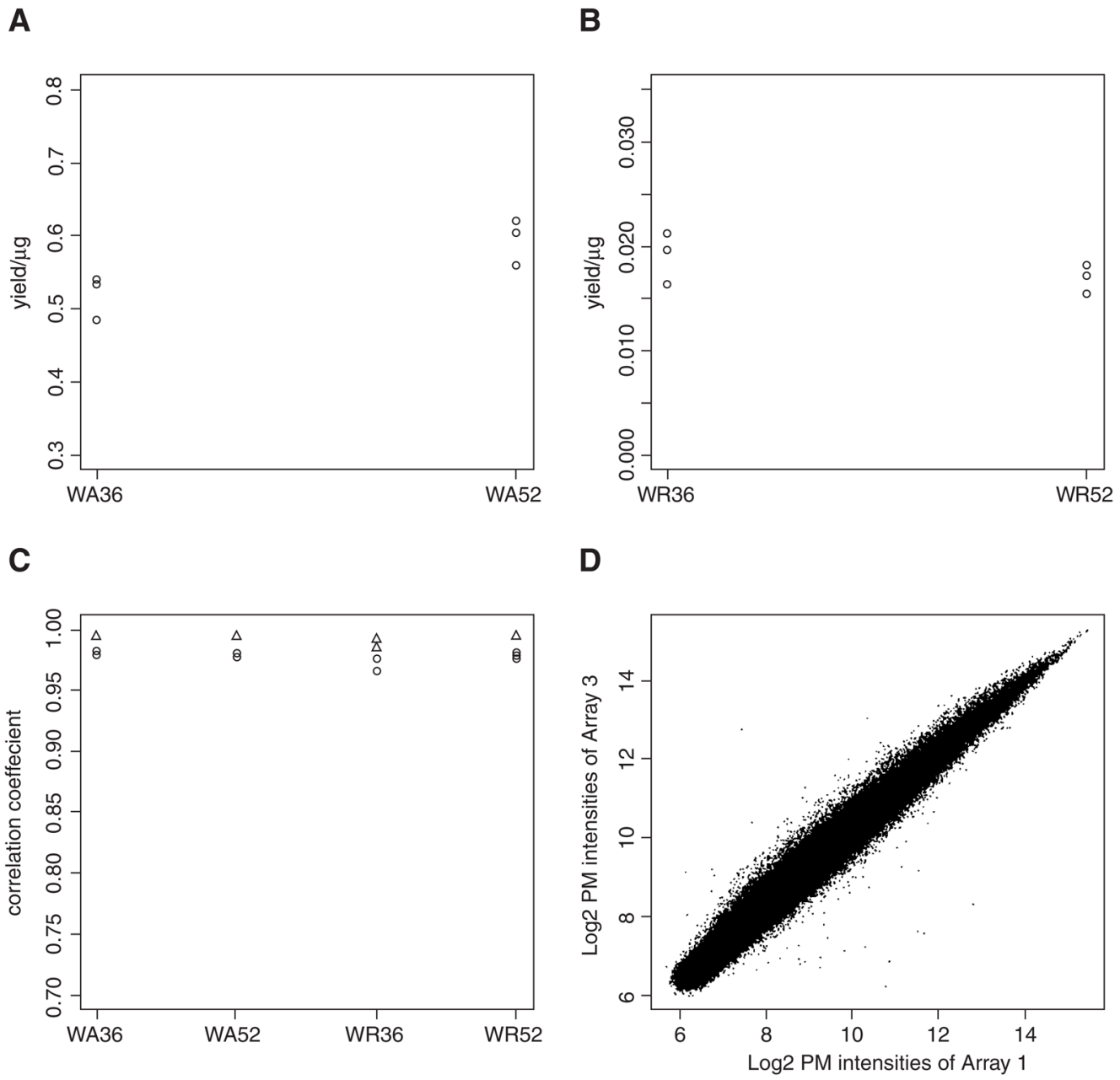

FIG. 5.

Total RNA yield and correlation of the biological replicates in the microarray study. (**A**) A dot plot of total RNA yield per embryo. (**B**) A dot plot of total RNA yield per retina. (**C**) A dot plot of pairwise correlation coefficients among the three biological replicates of same type of sample, using PM probe intensities *(circles)* and normalized intensities *(triangles)* of the microarray experiments. (**D**) A scatterplot of PM probe intensities of the microarray result between biological replicate 1 and 3 of WA36. WA36: wild-type embryo sample collected at 36 hpf. WA52: wild-type embryo sample collected at 52 hpf. WR36: wild-type retinal sample collected at 36 hpf. WR52: wild-type retinal sample collected at 52 hpf.

NIH-PA Author Manuscript NIH-PA Author Manuscript NIH-PA Author Manuscript

Table 1

Top Twenty Over- and Under-expressed Annotated Genes in the Wild-type Retinal Samples Compared to the Whole-Embryo Samples at 52hpf (WR52/WA52), and the Corresponding Comparisons of Retinal Samples at 52 and 36hpf (WR52/WR36).

Top twenty over-expressed annotated genes

mbol	Gene title	Fold change at 52 hpf (WR52/ WA52)	Corresponding retinal fold Change Compared with 36 hpf (WR52/WR36)	GO biological process	GO cellular component	GO molecular function	zfin ID
	guanylate kinase 1	15.27	18.8	transport	intracellular	ATP binding; kinase activity	ZDB-GENE-020916-1
	Recoverin	13.54	42.11	—	—	calcium ion binding	ZDB-GENE-030131-7590
	prominin-like 2	10.41	30.38	—	integral to membrane	—	ZDB-GENE 031003-1
	rad and gem related GTP binding protein 1	8.76	9.82	small GTPase mediated signal transduction	—	GTP binding	ZDB-GENE-040317-1
	paired box gene 6b	8.24	1.49	transcription; regulation of transcription, DNA-dependent development	nucleus	DNA binding; transcription factor activity	ZDB-GENE-001031-1
	elongation of very long chain fatty acids (FEN1/Elo2, SUR4/Elo3, yeast)-like 1	8.14	13.65	—	integral to membrane	—	ZDB-GENE-030131-7672
	retinaldehyde binding protein 1, like	7.64	6.09	transport	intracellular	transporter activity	ZDB-GENE-040426-1662
	sine oculis homeobox homolog 7	7.61	5.51	regulation of transcription, DNA-dependent; development	nucleus	DNA binding; transcription factor activity	ZDB-GENE-990825-28
	N-myc downstream regulated gene 1, like	7.59	3.19	cell differentiation	—	catalytic activity	ZDB-GENE-040426-1648
	rhodopsin	6.97	10.51	G-protein coupled receptor protein signaling pathway; visual perception; photo-transduction; rhodopsin mediated phototransduction	integral to membrane	rhodopsin-like receptor activity; receptor activity; G-protein coupled receptor activity; G-protein coupled photoreceptor activity; photoreceptor activity; retinal binding	ZDB-GENE-990415-271
	arylalkylamine N-acetyltransferase	6.89	7.88	response to photoperiod	—	aralkylamine N-acetyltransferase activity; N-acetyltransferase activity; acyltransferase activity; transferase activity	ZDB-GENE-991019-6
	guanine nucleotide binding protein (G protein), gamma transducing activity polypeptide 2	6.87	6.58	G-protein coupled receptor protein signaling pathway	Heterotrimeric G-protein complex	signal transducer activity	ZDB-GENE-030131-7595
	ADP-ribosylation factor-like 3, like 1	6.86	7.21	transport; intracellular protein transport; small GTPase mediated	Golgi apparatus	GTP binding	ZDB-GENE-040426-1649

Invest Ophthalmol Vis Sci. Author manuscript; available in PMC 2009 March 31.

NIH-PA Author Manuscript
NIH-PA Author Manuscript
NIH-PA Author Manuscript

Top twenty over-expressed annotated genes

mbol	Gene title	Fold change at 52 hpf (WR52/ WA52)	Corresponding retinal fold Change Compared with 36 hpf (WR52/WR36)	GO biological process	GO cellular component	GO molecular function	zfin ID
				signal transduction; protein transport			
	atonal homolog 7	6.77	−2.40	regulation of cell cycle; eye morphogenesis; cell fate commitment; positive regulation of neurogenesis	—	—	ZDB-GENE-000926-1
	jun B proto-oncogene	6.65	5.73	regulation of transcription, DNA-dependent	nucleus	DNA binding	ZDB-GENE-040426-2172
	prospero-related homeobox gene 1	6.28	6.15	regulation of transcription, DNA-dependent; development; myofibril assembly; regulation of transcription	nucleus	DNA binding; transcription regulator activity	ZDB-GENE-980526-397
	visual system homeobox 1 protein	6.24	4.41	regulation of transcription, DNA-dependent; development; visual perception	nucleus	DNA binding; transcription factor activity	ZDB-GENE-990415-205
	carbonic anhydrase VII	6.05	4.99	one-carbon compound metabolism	—	carbonate dehydratase activity; zinc ion binding; lyase activity	ZDB-GENE-040426-1786
	retinal homeobox gene 3	6.02	6.00	eye morphogenesis; regulation of transcription, DNA-dependent; development	nucleus	DNA binding; transcription factor activity	ZDB-GENE-990415-238
	Top twenty under-expressed annotated genes						
	myosin, heavy polypeptide 2, fast muscle specific	−745.22	1.04	muscle development	cytoskeleton; myosin	motor activity; actin binding; ATP binding;	ZDB-GENE-020604-1
	fast muscle troponin I	−383.09	−1.21	—	—	—	ZDB-GENE-040625-119[1]
	ATPase, Ca^{++} transporting, cardiac muscle, fast twitch 1	−380.55	−1.16	cation transport; calcium ion transport; calcium ion homeostasis; regulation of muscle contraction; metabolism; response to mechanical stimulus; proton transport; negative regulation of muscle contraction	membrane; integral to membrane	catalytic activity; calcium-transporting ATPase activity; ATP binding; APTase activity, coupled to transmembrane movement of ions, phosphorylative mechanism; hydrolase activity, acting on acid anhydrides, catalyzing transmembrane movement of substances	ZDB-GENE-020905-1
	ictacalcin	−337.9	−1.15	—	—	calcium ion binding	ZDB-GENE-030131-8599
	troponin C, fast skeletal	−328.12	−1.13	ciliary or flagellar motility	flagellum (sensu Bacteria)	calcium ion binding	ZDB-GENE-000322-2

Invest Ophthalmol Vis Sci. Author manuscript; available in PMC 2009 March 1.

NIH-PA Author Manuscript
NIH-PA Author Manuscript
NIH-PA Author Manuscript

Top twenty over-expressed annotated genes

mbol	Gene title	Fold change at 52 hpf (WR52/ WA52)	Corresponding retinal fold Change Compared with 36 hpf (WR52/WR36)	GO biological process	GO cellular component	GO molecular function	zfin ID
	troponin T3b, skeletal, fast	−283.19	−1.18	muscle development	muscle fiber	—	ZDB-GENE-030520-2
	slow skeletal myosin heavy chain 5	−283.09	−1.22	—	—	—	—
	periostin, osteoblast specific factor	−232.39	−3.05	cell adhesion; muscle attachment	—	—	ZDB-GENE-030131-9120
	actin, alpha 1, skeletal muscle	−223.98	−1	—	actin filament; actin cytoskeleton	motor activity; structural molecule activity; structural constituent of cytoskeleton	ZDB-GENE-000322-1
	parvalbumin, like	−200.45	−1.03	muscle development	—	calcium ion binding	ZDB-GENE-000322-4
	type 1 cytokeratin, enveloping layer	−197.48	1.19	—	intermediate filament	structural molecule activity	ZDB-GENE-991008-6
	transferrin a	−184.61	1.46	transport; iron ion transport; iron ion homeostasis	extracellular region	ferric iron binding	ZDB-GENE-980526-35
	keratin 4	−179.16	−1.15	—	intermediate filament	structural molecule activity	ZDB-GENE-000607-83
	troponin T3a, skeletal, fast	−177.74	−1.26	muscle development	muscle fiber	—	ZDB-GENE-000322-3
	cofilin 1 (non-muscle)	−167.33	−1.30	—	intracellular	actin binding	ZDB-GENE 040426-2770
	collagen, type I, alpha 1	−163.32	−1.45	phosphate transport; regulation of ossification	extracellular matrix (sensu Metazoa); collagen); cytoplasm	structural molecule activity; extracellular matrix structural constituent	ZDB-GENE-030131-9102
	claudin i	−156.27	−1.07	—	tight junction; membrane; integral to membrane	structural molecule activity	ZDB-GENE-010328-9
	retinol binding protein 4, plasma	−155.84	−1.27	transport	—	transporter activity; retinoid binding	ZDB-GENE-000210-19
	creatinine kinase, muscle	−131.63	1.83	—	—	actin binding; kinase activity; transferase activity; transferring phosphorus-containing groups	ZDB-GENE-980526-109
	alpha-tropomyosin	−120.76	1.66	muscle development	cytoskeleton	actin binding	ZDB-GENE-990415-269

Ontology.

no *Tnni2* in zfin as of July 2005, but there is an unannotated clone having the same ZGC ID.

Invest Ophthalmol Vis Sci. Author manuscript; available in PMC 2009 March 31.